Title
Estrogen-responsive nitroso-proteome in uterine artery endothelial cells: Role of endothelial nitric oxide synthase and estrogen receptor-β

Journal
Journal of Cellular Physiology, 227(1)

ISSN
0021-9541

Authors
Zhang, Hong-hai
Feng, Lin
Wang, Wen
et al.

Publication Date
2012

DOI
10.1002/jcp.22712

Peer reviewed

Published in final edited form as:
J Cell Physiol. 2012 January ; 227(1): 146–159. doi:10.1002/jcp.22712.

Estrogen-Responsive *nitroso*-Proteome in Uterine Artery Endothelial Cells: Role of Endothelial Nitric Oxide Synthase and Estrogen Receptor-β

Hong-hai Zhang[1], **Lin Feng**[1], **Wen Wang**[1], **Ronald R. Magness**[3], and **Dong-bao Chen**[1,2]

[1]Department of Obstetrics & Gynecology, University of California-Irvine, Irvine, CA 92697

[2]Experimental Pathology, University of California-Irvine, Irvine, CA 92697

[3]Department of Obstetrics and Gynecology - Perinatal Research Laboratories, University of Wisconsin-Madison, Madison, WI 53715

Abstract

Covalent adduction of a NO moiety to cysteines (*S*-nitrosylation or SNO) is a major route for NO to directly regulate protein functions. In uterine artery endothelial cells (UAEC), estradiol-17β (E2) rapidly stimulated protein SNO that maximized within 10-30 min *post*-E2 exposure. E2-bovine serum albumin stimulated protein SNO similarly. Stimulation of SNO by both was blocked by ICI 182, 780, implicating mechanisms linked to specific estrogen receptors (ERs) localized on the plasma membrane. E2-induced protein SNO was attenuated by selective ERβ, but not ERα, antagonists. A specific ERβ but not ERα agonist was able to induce protein SNO. Overexpression of ERβ, but not ERα, significantly enhanced E2-induced SNO. Overexpression of both ERs increased basal SNO, but did not further enhance E2-stimulated SNO. E2-induced SNO was inhibited by *N*-nitro-L-arginine-methylester and specific endothelial NO synthase (eNOS) siRNA. Thus, estrogen-induced SNO is mediated by endogenous NO via eNOS and mainly ERβ in UAEC. We further analyzed the *nitroso*-proteomes by CyDye switch technique combined with two dimensional (2D) fluorescence difference gel electrophoresis. Numerous nitrosoprotein (spots) were visible on the 2D gel. Sixty spots were chosen and subjected to matrix-assisted laser desorption/ionization-time of flight mass spectrometry. Among the 54 identified, 9 were novel *SNO*-proteins, 32 were increased, 8 were decreased, and the rest were unchanged by E2. Tandom MS identified Cys139 as a specific site for SNO in GAPDH. Pathway analysis of basal and estrogen-responsive *nitroso*-proteomes suggested that SNO regulates diverse protein functions, directly implicating SNO as a novel mechanism for estrogen to regulate uterine endothelial function and thus uterine vasodilatation.

Keywords

Estrogen; nitric oxide; *S*-nitrosylation; proteomics; uterine artery endothelial cells

Introduction

Estrogens are potent vasoactive agents that dilate various vascular beds throughout the body, with the greatest response occurring in the uterus (Magness and Rosenfeld, 1989; Markee,

Address correspondence to: Dong-bao Chen, Ph.D., Department of Obstetrics and Gynecology, University of California Irvine, Irvine, CA 92697. dongbaoc@uci.edu.

Disclosure: The authors have nothing to disclose.

1932). In ovariectomized and intact animals, following estrogen administration uterine vasodilatation as measured by a rise in uterine blood flow (UBF) begins to increase within 30-45 minutes and reaches up to 10-fold baseline within 90-120 minutes (Magness and Rosenfeld, 1989). The stimulatory effect of estrogens on UBF has been verified under physiological statuses linked to increased levels of circulating estrogens such as the follicular phase of the ovarian cycle and pregnancy, in which UBF has been shown to be significantly elevated (Ford, 1982; Gibson et al., 2004; Magness et al,. 2005). Of note, during the last one third of gestation dramatic rise in UBF is directly linked to fetal growth and insufficient rise in UBF results in intrauterine growth restriction and other serious obstetric problems (Lang et al., 2003).

Numerous studies have shown that estrogen-induced uterine vasodilatation is largely mediated by nitric oxide (NO) synthesized via endothelial NO synthase (eNOS) locally in the uterine artery endothelial cells (UAEC) (Chen et al., 2006; Magness et al., 2001; Rosenfeld et al., 1996; Rupnow et al., 2001). We have shown that estradiol-17β (E2) stimulates rapid NO production independent of *de novo* eNOS synthesis in UAEC (Chen et al., 2004). Chronic estrogen treatment stimulates uterine artery endothelial eNOS expression similarly as shown in other vascular beds (Chen et al., 2006; Rupnow et al., 2001; Vagnoni et al., 1998). The rapid activation and latent rises in expression of eNOS protein in endothelial cells (ECs) on estrogen stimulation are thought to be mediated by specific estrogen receptors (ER) localized either on the plasma membrane (Chen et al., 2004; Liao et al., 2005) or in the nucleus (Truss and Beato, 1993). However, despite extensive studies showing estrogen stimulation of endothelial NO production in the uterine arteries, the direct effects of enhanced NO by estrogen stimulation in the endothelium itself has not yet being explored.

The classical route for NO to elicit its biological functions is the formation of cyclic guanylate monophosphate (cGMP) that is important for vascular remodeling, vessel relaxation and platelet aggregation, etc (Murad, 1986). However, NO also possesses many bioactivities that are cGMP independent (Wanstall et al., 2005). Covalent adduction of a NO moiety ($NO^{\bullet}$) to cysteines defined as *S*-nitrosylation (SNO) represents a major mechanism for NO to directly regulate protein functions (Stamler et al., 1992a). More recently, SNO has been rapidly moving to “the center stage” of cell signaling and its physiological significance has been regarded as homolog to *O*-phosphorylation (Lane et al., 2001). SNO is a novel pathway for *post*-translational modification of proteins. This redox sensitive change in NO moiety alters the functions of nearly all major classes of proteins, thus inevitably participating in a plethora of important biological pathways including apoptosis, redox signaling, and angiogenesis, etc (Hess et al., 2005).

Uterine artery endothelial NO production plays a critical role in mediating estrogen stimulation of uterine vasodilatation linked to specific ER, i.e., ERα and ERβ (Liao et al., 2005; Byers et al., 2005; Magness et al., 2005); however, it is unknown to date if estrogens directly regulate endothelial protein SNO in UAEC via a specific ER-subtype mediated mechanism. In this study, we have used a comprehensive proteomics approach to investigate the effects of estrogens on protein SNO in primary UAEC. We reported herein for the first time that estrogen stimulates dynamic protein SNO in UAEC, which is linked to endogenous NO via eNOS and ERβ. Pathway analysis of the *SNO*-proteins identified in the resting and estrogen-treated UAEC revealed that protein SNO regulates diverse biological functions. Our findings hence implicate SNO as a novel mechanism for estrogens to regulate uterine endothelial function and thus vasodilatation.

Materials and Methods

Chemicals and antibodies

Estradiol-17β, β-estradiol 6-(*O*-carboxymethyl)oxime-bovine serum albumin (E2-BSA), sodium ascorbate, N-2-Hydroxyethylpiperazine-N′-2-ethanesulfonic acid (HEPES), diethylene triamine pentaacetic acid (DTPA), neocuproine, mercury chloride, copper chloride, fatty acid free bovine serum albumin (BSA), *N*-nitro-L-arginine-methylester (L-NAME), *N*-nitro-D-arginine-methylester (D-NAME), methanol, N-ethylmeleimide (NEM), methyl methanethiosulfonate (MMTS), 3-(3-Cholamidopropyl)dimethylammonio-1-propanesulfonate (CHAPS), sodium dodecyl sulfate (SDS), dimethyl sulfoxide (DMSO) and all other chemicals unless specified, were from Sigma (St Louis, MO). *N*-[6-(biotinamido)hexyl]-3′-(2′-pyridyldithio) propionamide (biotin-HPDP) were from Thermo scientific (Rockford, IL). ICI 182, 780, 1,3-Bis(4-hydroxyphenyl)-4-methyl-5-[4-(2-piperidinylet hoxy)phenol]-1H-pyrazole dihydrochloride (MPP), 4-[2-Phenyl-5,7-bis(trifluoromethyl)pyrazolo[1,5-a]pyrimidin-3-yl]phenol (PHTPP), 4,4,4-(4-propyl-[1H]-pyrazole-1,3,5-triyl)trisphenol (PPT), diarylpropionitrile (DPN) were from Tocris (Ellisville, MO). S-nitrosoglutathione (GSNO) was from Cayman (Ann Arbor, MI). Anti-biotin antibody was from Cell Signaling Technology (Beverly, MA). 2-(6-biotinoyl-amino-hexanoyl amino) ethylmethanethiosulfonate (MTSEA)-Texas red was from Toronto Research Chemicals (Downsview, ON, Canada). Cydye DIGE fluor labeling kit was from GE Healthcare (Buckinghamshire, UK). Anti-β-actin monoclonal antibody was from Ambion (Austin, TX). Anti-ERα antibody was from Neomarkers (Fremont, CA). Anti-ERβ antibody was from Affinity Bioreagents (Rockford, IL). Anti-eNOS antibody was from Santa Cruz Biotechnology, Inc (Santa Cruz, CA). Prolong Gold antifade reagent with 4′,6-diamidino-2-phenylindole (DAPI), MCDB131 and M199 were from Invitrogen (Carlsbad, CA).

Cell culture

UAEC were isolated by collagenase digestion from late pregnant (D120-130 days of gestation, term ≈145 days) ewes as described previously (Bird et al., 2000). The animal use protocol was approved by the Animal Subjects Committees of the University of California San Diego and the University of Wisconsin-Madison. Frozen UAEC aliquots (passage 3) were thawed and seeded in MCDB131 containing 10% fetal bovine serum (Lonza, Walkersville, MD) and antibiotics for experimental use at passages 4–5. Cells at ~70% confluence were cultured in serum-free M-199 (Phenol red-free M-199 containing 0.1% fatty acid-free BSA and 25 mM HEPES) for 16 h. Following 1 h equilibration in fresh serum-free M-199 medium with or without inhibitors as indicated in the figure legends, UAEC were treated without or with E2 for various times in the presence or absence of L-NAME or ICI 182, 780. Ethanol was used to dissolve E2 and ER antagonists; its final concentration was <0.01% that did not alter cellular responses surveyed in this study.

Small interfering RNA (siRNA) knockdown of eNOS

An eNOS siRNA based on the sequence (5′-GAGTTACAAGATCCGCTTCdTdT-3′, positioned at 1824–1842) of the open reading frame of bovine eNOS (Kang-Decker et al., 2007) was synthesized by Dharmacon (Lafayette, CO). A nonspecific siRNA (5′-AUUGUAUGCGAUCGCAGACdTdT-3′) from Dharmacon was used as a negative control. Transfection of siRNA into UAEC was performed with RNAiMAX reagent (Invitrogen, Carlsbad, CA) following the manufacturer's protocol with a final concentration of 200 nM. Forty-eight hours post-transfection, UAEC were cultured in serum-free M-199 medium for 6 h for experimental use.

Adenoviral overexpression of ERα and ERβ

Replication-defective adenovirus expressing full length wild-type human ERα (Ad5ERα) and ERβ (Ad5ERβ) were kindly provided by Dr. Mark J. Evans (Evans et al., 2002). UAEC were seeded in MCDB131 containing 10% FBS. When cells reached to ~50% confluence, medium was changed to Phenol red-free M-199 containing 1% FBS with or without Ad5ERα, Ad5ERβ, or both at an approximate multiplicity of infection (MOI) of 50 or 500, respectively. After 6h viral infection, the cells were cultured in MCDB131 containing 10% FBS and antibiotics for 24 h, followed by serum-free M-199 medium overnight. Infected cells were then subject to E2 treatment.

Biotin-switch method (BST) and avidin capture of nitrosopoteins

Biotin switch was preformed as previously described (Jaffrey and Snyder, 2001; Zhang et al., 2010). Briefly, UAEC (~4×10^6 cells) were lysed in blocking buffer (25 mM HEPES, pH 7.7, 1 mM DTPA, 0.1 mM neocuproine, 0.4% CHAPS, 50mM NEM and 2.5% SDS). Protein content of the samples was determined and all samples were adjusted to 0.6 mg/ml. The samples (50 μg/group) were transferred to 1.5-ml amber Eppendorf tubes and were incubated at 50°C in dark for 30 min, followed by precipitation with cooled (-20°C) acetone (1:3, vol/vol) and incubation at -20°C for 2 h. Following centrifugation (12,000×g, 10 min), the acetone precipitated proteins (pellets) were washed once with 75% cold acetone, then resuspended in labeling buffer (25 mM HEPES, pH 7.7, 30 mM sodium ascorbate, 0.1 μM $CuCl_2$, 0.4 mM biotin-HPDP and 1% SDS). After adjusting protein content to 0.6mg/ml, the samples were incubated at 37°C in dark for 1 h with occasional agitation. The samples were then mixed with SDS sample buffer (without DTT or 2-Mercaptoethanol), and used for immunoblotting as below.

To analyze specific *SNO*-proteins, the biotin-labeled samples (~0.25 mg) were mixed with 50 μl of NeutrAvidin™ Protein coated beads (Thermo scientific, Rockford, IL) and incubated at 4°C overnight. The avidin captured biotinylated proteins were eluted from the beads with 100 μl of 1× SDS sample buffer with 0.1 M 2-Mercaptoethenol at 37°C for 20 min, and then used for immunoblotting.

SDS-PAGE and immunoblotting for *SNO*-proteins

Proteins were separated on 8-12% SDS-PAGE, and transferred onto polyvinylidene fluoride membranes as described previously (Liao et al., 2009). Total *SNO*-proteins for each sample were detected by immunoblotting with anti-biotin antibody. All *SNO*-proteins in each lane was summed for the level of *SNO*-proteins of the sample. Individual *SNO*-protein was measured by immunoblotting of the avidin captured *SNO*-proteins by specific antibody.

Detection of *SNO*-proteins in intact cells by fluorescence microscopy

SNO-proteins were detected in intact cells by a modified BST protocol as previously described (Zhang et al., 2010). Briefly UAEC were cultured on glass coverslips and cultured in serum free M-199 when reaching 70% confluence and treated with E2 with or without inhibitors. The cells were washed with cold phosphate buffered saline (PBS) and fixed with methanol at -20°C for 15 min. Free thiols were blocked with 0.2 M MMTS in HEN/ methanol buffer (80% methanol, 100 mM HEPES, pH 7.7, 1 mM EDTA, and 0.1 mM neocuproine) at 50°C for 30 min in dark. After 3 washes with 100 mM HEPES/80% methanol, the cells were incubated with 0.2 M ascorbate and 0.2 μM MTSEA-Texas Red in 100 mM HEPES/80% methanol in dark at 37°C for 1h. After extensive washing with the methanol, the cells were mounted with Prolong Gold antifade reagent with DAPI and examined under a fluorescence microscope (Leica, Wetzlar, Germany) for image acquisition and captured by a Hamamatsu CCD camera using the *SimplePCI* software.

CyDye switch labeling and two-dimensional fluorescence difference gel electrophoresis (2D-DIGE)

Cydye switch labeling based on the biotin switch technique was performed as previously described (Zhang et al., 2010). Briefly, after blocking free thiols in cell lysates (100 μg protein/sample) in blocking buffer, acetone precipitated proteins were resuspended in 35 μl of reducing buffer (30 mM Tris-HCl, pH 8.0, 7 M urea, 2 M thiourea, 4% CHAPS) containing 30 mM sodium ascorbate and 0.1 μM Copper(II) Chloride and incubated in dark at 37°C for 1 h. CyDye DIGE Fluor Cy3 or Cy5 saturation dye (4 μl, 2 mM) were added into control or E2-treated samples, respectively. The samples were incubated in dark at 37°C for 30 min. The reaction was stopped by addition of 35 μl of 2× 2D-Sample buffer (7 M urea, 2 M thiourea, 4% CHAPS, 2% pharmalytes 3-10, 130 mM dithiothreitol) and stored at -80°C for 2D-DIGE. To prevent the disulfide (S-S) bond being reduced to free thiols (-SH) during the CyDye labeling process as described in the standard protocol for CyDye saturation labeling, the reducing agent tris-[2-carboxyethyl]-phosphine (TCEP) was not added.

2D-DIGE was performed by Applied Biomics, Inc (Hayward, CA). Just prior to 2D-DIGE, equal amounts of Cy3- and Cy5-labeled samples (50 μg each) were mixed with rehydration buffer. After adding de-streak solution (GE Healthcare, UK) and 1% pH 3-10 pharmalyte (GE Healthcare, UK), the samples were loaded onto an IEF strip (pH 3-10 linear range, GE Healthcare, UK). IEF was done for a total of 25,000 V-h with standard conditions using Ettan IPGPhore II. After the IEF, electrophoresis was performed at 16°C on 10% SDS-PAGE. The resulting 2-D gel was scanned using a Typhoon Trio scanner (GE Healthcare, UK) with excitation and emission wavelengths for Cy3-labelled (548/560 nm) and Cy5-labelled (641/660 nm) protein with settings that Cy3 or Cy5 labeled same samples resulted in similar relative red or green fluorescence intensities. Image analysis for intensity measurement of protein spots chosen was performed using the *ImageQuant* and *DeCyder* software (GE Healthcare, UK).

Protein identification by matrix-assisted laser desorption/ionization-time of flight (MALDI-TOF) and tandem mass spectrometry (MS)

Protein identification was performed by Applied Biomics, Inc (Hayward, CA). After analyses of the 2D-DIGE image, selected protein spots of interest (based on intensity and visibility) were picked up from the gel using Ettan spot picker (GE Healthcare, UK). Each individual sample was washed twice with 25 mM ammonium bicarbonate and 50% acetonitrile to remove staining dye, once with water and once with 100% acetonitrile. The samples were dried and rehydrated in digestion buffer (25 mM ammonium bicarbonate, 2% acetonitrile) containing 0.5% sequencing grade trypsin (Promega, Madison, MI). Proteins were digested in-gel at 37°C overnight. Digested peptides were extracted with TFA extraction buffer (0.1% trifluoroacetic acid). The digested tryptic peptides were desalted using C-18 Zip-tips (Millipore, Billerica, MA) and then mixed with alpha-cyano-4-hydroxycinnamic acid (CHCA) matrix and spotted into wells of a MALDI plate. Mass spectra of the peptides in each digested spot were obtained by using an Applied Biosystems 4700 Proteomics Analyzer (Applied Biosystems, Foster City, CA). Ten to twenty of the most abundant peptides in each sample were further subjected to fragmentation and MS/MS analysis. Identification of each sample (2D spot) was searched based on peptide fingerprinting MS spectra and peptide fragmentation MS/MS spectra. Combined MS and MS/MS spectra were submitted for database search using GPS Explorer software (Applied Biosystems, Foster City, CA) equipped with the MASCOT search engine (http://www.matrixscience.com) to identify proteins from National Center Biotechnology Information non-redundant *Bos Taurus* and *Ovis aries* amino acid sequence database with oxidation and carbamidomethy and phosphorylation as variable modifications. The highest

protein scoring hit with a protein score confidence interval over 95% from the database search for each 2D gel spot was accepted as positive identification.

Identification of nitrosylated cysteines by mass spectrometry and database search

Once a *SNO*-protein was identified according to the MS spectra of its tryptic peptides, a monoisotopic mass shift (Cy3: 672.2981 Dalton or Cy5: 684.2981 Dalton) was applied to the MS spectra for identifying specific cysteines nitrosylated by using the MASCOT algorithm. The shifted peaks were located in the spectra and subjected to MS/MS. Since cysteine-CyDye Labeling is not included as peptide modification in any amino acid sequence databases, identification of each peptide was based on fragmentation MS/MS spectral comparisons with theoretical spectra manually. A positive identification was defined by over 10 observed fragmental masses matched with a theoretical one.

Pathway analysis and statistics

Ingenuity pathway analysis tool (www.ingenuity.com, Ingenuity Systems, Redwood City, CA) was used for pathway analysis of the identified *SNO*-proteins. Positive result was defined as -log (p-value) more than 1.30 ($P < 0.05$). Statistics were performed using *Sigma*Stat 3.5 (*Systat* Software Inc., San Jose, CA). Data were analyzed by ANOVA, followed by LSD test for comparisons between estrogen treatments vs. control. Significance was defined as $P < 0.05$.

Results

E2 stimulates protein SNO UAEC in a time- and concentration- dependent manner

When the *SNO*-proteins were labeled with biotin by BST and measured by immunoblotting with an anti-biotin antibody, basal levels of various *SNO*-proteins separated on SDS-PAGE were readily detectable. Treatment with E2 stimulated total levels of *SNO*-proteins in a time- and concentration-dependent fashion. Following E2 treatment, total levels of *SNO*-proteins rapidly increased at 2 min, maximized around 15-30 min, and returned to baseline after 60 min (Fig. 1A). When treated with 0.1 nM to 1 μM E2 for 30 min, both 10 and 100 nM E2 significantly stimulated total levels of *SNO*-proteins (Fig. 1B).

E2 stimulation of protein SNO is mediated by endogenous NO via eNOS

Estrogen stimulation of endothelial NO production has been well documented and we have shown that estrogen stimulates rapid NO production via mitogen-activated protein kinase dependent eNOS activation in UAEC (Chen et al., 2004); this raises a question whether E2-induced endothelial protein SNO is mediated by endogenous NO. To address this, we tested the effects of E2 on protein SNO in UAEC pretreated with or without a specific NOS inhibitor L-NAME (1 μM) or its inactive stereo isoform D-NAME. L-NAME, but not D-NAME, completely abolished E2 stimulated SNO (Fig. 2A). Since eNOS is the dominant NOS isoform for synthesizing NO in ECs (Bird et al., 2000; Forstermann et al., 1998; Magness et al., 1997; Vagnoni et al., 1998), we further tested the role of eNOS in E2-induced SNO. When UAEC was transfected with a specific eNOS siRNA, but not a control siRNA, eNOS protein was reduced by 90%. In eNOS siRNA, but not control, siRNA transfected UAEC, E2-induced SNO was completely inhibited (Fig. 2B). These findings clearly demonstrate that E2 induced SNO requires endogenous NO derived from eNOS in UAEC. These findings were then verified with a modified BST (Fig 2C) by using a fluorescent tag for visualizing *SNO*-proteins in intact cells. Basal MTSEA-Texas-Red labeled *SNO*-proteins were detected in methanol-fixed UAEC. Treatment with E2 (10 nM, 30 min) increased the labeling intensity (indicative *SNO*-proteins). Pretreatment with L-

NAME, but not D-NAME, drastically lowered the labeling intensity on E2 stimulation (Fig. 2C).

E2 stimulation of protein SNO is mediated mainly by ERβ

Both ERα and ERβ are expressed in UAEC (Byers et al., 2005; Jobe et al., 2010; Liao et al., 2005), raising a question as to their specific roles in estrogen stimulation of protein SNO in UAEC. To this end, we pretreated UAEC with or without a pure but nonselective ER antagonist ICI 182,780 (1 μM) for 1 h, and then determined the effects of E2 on protein SNO. Compared to controls, ICI 182,780 alone did not alter total *SNO*-protein levels. In the presence of ICI 182,780, however, E2 stimulation of protein SNO was blocked (Fig 3). Since estrogen induced protein SNO within minutes (Fig. 1), suggesting non-classical rapid "non-genomic" action possibly mediated by receptors on plasma membrane, we tested the effects of a cell-impermeable estrogen compound E2-BSA on protein SNO in the presence or absence of ICI 182,780. Treatment with 10 nM E2-BSA for 30 min significantly stimulated total levels of *SNO*-proteins; similar to E2 treatment alone, the E2-BSA-induced SNO was blocked by ICI 182,780 (Fig. 3A). These results were confirmed by *in situ SNO*-protein detection with MTSEA-Texas-Red labeling (Fig. 3B).

To determine the specific roles of ERα and ERβ, we used an adenoviral system to selectively overexpress ERα, ERβ, or both in UAEC. High levels of ERα or ERβ were detected in UAEC infected with AdERα or AdERβ, respectively; when cells were infected with both AdERα and AdERβ, comparable high levels of both ERα and ERβ proteins were detected. Treatment with E2 increased the level of *SNO*-proteins in UAEC infected with control adenovirus carrying green fluorescence protein (GFP). Of note, the overexpressed GFP were readily S-nitrosylated in both UAEC with and without E2 treatment (Fig. 4A). In comparison with GFP overexpressed controls, overexpression of ERβ, but not ERα, significantly enhanced the total level of E2-induced *SNO*-proteins that excluded *SNO*-GFP (Fig. 4A). Overexpression of both ERα and ERβ increased baseline of *SNO*-proteins in UAEC; however, it did not further enhance E2-induced SNO. Specific antagonists of ERα (MPP) and ERβ (PHTPP) were used to further consolidate this conclusion. In the presence of PHTPP or in combination of MPP, but not MPP alone, E2-induced SNO proteins was attenuated in UAEC (Fig. 4B). Moreover, the selective agonists of ERα (PPT) and ERβ (DPN) were used to further delineate the role of specific ERs. Treatment with DPN but not PPT significantly induced SNO in UAEC (Fig. 4C). These findings demonstrate that ERβ is the primary receptor that mediates E2-induced SNO in UAEC and that ERα may help to partially facilitate these actions with a small subset of proteins.

Cyde Switch, 2D-DIGE analysis of estrogen regulated endothelial *nitroso*-proteome

As only a limited number (~20) of *SNO*-proteins can be separated on SDS-PAGE and visualized by immunoblotting with anti-biotin antibody, to fully analyze estrogen-regulated *nitroso*-proteome we recently established the much more powerful proteomics approach 2D-DIGE to separate the *SNO*-proteins (Zhang et al., 2010). First, in the BST procedure fluorescent CyDye flours were used to replace the biotin tag for labeling *SNO*-proteins in control (labeled with Cy3, green) and E2 (labeled with Cy5, red) treated UAEC, respectively. After the samples were labeled with BST using CyDye (termed as CyDye switch), protein concentrations in the samples were re-determined. Equal amounts of total proteins (50 μg/group) from control and E2 treated cells were mixed and then separated on a 2D analytic gel. Following 2D electrophoresis, the resulting gel was scanned in both Cy3 and Cy5 channels and relative fluorescence intensities were calculated as a ratio between control and E2 for the spots chosen (Table 1).

We achieved very similar results of the *nitroso*-proteomes in control and E2-treated UAEC isolated from three different pregnant ewes (Supplemental Fig. 1). A representative merged 2D-DIGE image of the resting and E2-responsive *nitroso*-proteomes is shown in Fig. 5. Approximately 1000 fluorescent spots are visible on the 2D-gel, which should be all *SNO*-proteins. Notably, many proteins were readily nitrosylated under resting conditions. Treatment with E2 (10 nM, 30 min) significantly altered the *nitroso*-proteome in UAEC; E2 treatment increased the levels of many *SNO*-proteins (red spots) but also unexpectedly decreased some others (green spots) that were unable to detect on SDS-PAGE. The rest (yellow spots) were unchanged by E2.

Identification of *SNO*-proteins in UAEC by MALDI-TOF MS

According to the intensity and visibility of the spots on the analytic 2D-DIGE image, the ratios between the intensities of the relative levels of the *SNO*-proteins in E2-treated and control cells were determined for the spots as listed in Table 1. Ratios greater than 1 and with $P < 0.05$ represented spots up-regulated by E2; while ratios ranging from 0 to 1 and with $P<0.05$ represented spots decreased by E2. Based on these data, 200 μg total proteins of both control and E2-treated samples were prepared by CyDye switch and run on a preparative 2D DIGE. After image acquisition, spots were matched with the analytic gel. The spots on the new gel same as chosen from the analytic gels were picked up. Each of the 60 spots obtained were trypsin digested and subjected to MELDI-TOF MS. Spot identification was performed based on the peptide fingerprinting MS/MS spectra with the MASCOT algorithm. With confidence interval greater than 95%, we identified 54 of the 60 spots. The identifications of these *SNO*-proteins were summarized in Table 1, in which ratios between the relative levels of all identified *SNO*-proteins were listed. All peptides matched for each of these spots were listed in Supplemental Table 1.

Glyceraldehyde-3-phosphate dehydrogenase (GAPDH) is one of the *SNO*-proteins identified in UAEC. It is an abundant enzyme required for glycolysis and participates in nuclear events including gene transcription, RNA transport and DNA replication (Sirover, 1999). SNO of GAPDH causes cell apoptosis (Hara et al., 2005). In the current study we focused specific interest to this target owing to these reported functions of *SNO*-GAPDH. We further developed a method to identify the specific cysteines of SNO in GAPDH by MALDI-TOF/MS. We observed a peptide of m/z=2390.1621 in agreement with the expected m/z value of IVSNASC^{139}TTNC^{143}LAPLAK, a cysteine-containing peptide in GAPDH (m/z=2390.1593, with mass shift of Cy5: 684.2981). Additional analysis of this peptide by MS/MS *de novo* sequence analysis using the MASCOT algorithm showed that Cys139 is one of the CyDye binding sites in GAPDH (Fig. 6C & D). In addition, comparable levels of *SNO*-GAPDH were detected in resting and E2-treated UAEC by 2D-DIGE (Spot 40, Fig. 6A) and immunoblotting of the avidin captured total *SNO*-proteins with specific anti-GAPDH antibody (Fig. 6B), implicating *SNO*-GAPDH is a stable *SNO*-protein in UAEC similar to that in rat brain (Paige et al., 2008). As a control, exogenous NO derived from GSNO did stimulated SNO of GAPDH in UAEC (Fig. 6B).

Pathway analysis of *SNO*-proteins in UAEC

Collectively, among the 54 *SNO*-proteins identified, 32 targets were significantly increased, 8 were decreased, and the rest were unchanged by E2 treatment. Pathway analysis suggested that theses *SNO*-proteins are linked to the regulation of basic cellular physiology including metabolism and molecular transport, cellular assembly and organization, signaling, protein modification, cell viability and proliferation, cell cycle, cellular movement, DNA replication/recombination/repair, gene expression, etc. Many *SNO*-proteins are enzymes that are critical for protein synthesis, folding, post-translational modification and degradation. Of note, 9 were novel *SNO*-proteins that had never been reported. Some house-keeping proteins

such as β-actin, Hsp60, cofilin-1, GAPDH, vimentin and annexin, were also identified as *SNO*-proteins. Of note, only a portion (~1/10) of the *nitroso*-proteome in UAEC observed on 2D gel was identified in this study. According to these data, apparently SNO plays a critical role in normal cell physiology and in response to E2 regulation in UAEC.

Discussion

We have investigated herein the effects of estrogens on SNO in the maternal artery derived UAEC by using a comprehensive proteomics approach based on the original BST (Jaffrey and Snyder, 2001). Our current study has demonstrated that E2-induced SNO requires endogenous NO derived from NOS because it was blocked by the NOS inhibitor L-NAME, consistent with the recent reports using HUVEC (Chakrabarti et al., 2010; Zhang et al., 2010). Our present study has further confirmed a critical role of eNOS as specific eNOS siRNA is able to completely attenuate E2-induced SNO in UAEC. Estrogen-induced SNO in both UAEC and HUVEC occurs within minutes, implicating a rapid “nongenomic” event that appears to be mediated by receptors localized on the plasma membrane. This is because: 1) the membrane impermeable E2-BSA stimulates SNO in HUVEC (Zhang et al., 2010) and UAEC within minutes (Fig. 1&3) and 2) both were blocked by ICI 182, 780. However, major differences between the two EC types also exist. In HUVEC estrogen-induced SNO seems to require both ERα and ERβ because: 1) neither ERα or ERβ agonist alone, but their combination, stimulated protein SNO; and 2) either ERα and ERβ antagonist blocked E2-induced protein SNO (Zhang et al., 2010). By contrast, in UAEC E2-induced SNO is primarily mediated by ERβ because: a) overexpression of ERβ, but not ERα, greatly enhanced E2-induced protein SNO and, b) the ERβ antagonist PHTPP, but not ERα antagonist MPP, blocked E2-induced protein SNO (Fig. 4). These findings demonstrate that the fetal vein-derived HUVEC and maternal artery-derived UAEC are different in terms of the mechanisms underlying estrogen stimulation of protein SNO. This is consistent with our previous study suggesting that estrogen activation of eNOS in UAEC only requires ERK2/1 (Chen et al., 2004); whereas in HUVEC Akt appears to be the protein kinase for mediating estrogen stimulation of eNOS activation (Haynes et al., 2000). Thus, our data have further strengthened the use of UAEC to be the suitable model for investigating estrogen-induced and pregnancy-associated uterine vasodilatation.

Consistent with our recent study in HUVEC (Zhang et al., 2010) and the current study in UAEC, many diverse proteins are readily nitrosylated in resting endothelial cells. These findings indicate that protein nitrosylation plays a critical role in the maintenance of numerous aspects of endothelial homeostasis. In this regard, the production of NO is one of most important physiologic activity of endothelial cells, which is clinically critical for vascular health. NO is an active gaseous molecule with a short half-life (~1 sec) (Smith et al., 2003). Once produced *in vivo*, it will be quickly converted to other more stable metabolites, including NO_2^-/NO_3^- and nitrosothiols (Radi et al., 2001; Stamler et al., 1992b; Zhang et al., 2011). The high levels of *SNO*-proteins in resting endothelial cells indicate that nitrosothiols including *SNO*-proteins accumulate in endothelial cells. Indeed, numerous *SNO*-proteins have been also reported to be stably nitrolsylated in tissues (Paige et al., 2008; Zhang et al., 2011). This is significant because the relative stable nitrosothiols can serve as a reservoir for bioavailable NO (Stamler et al., 1992b); when needed, NO can be released from this source to exert its function. The importance of SNO in vascular health has been clearly implicated in the phenotypes of mice lacking the major *S*-nitrosoglutathione (GSNO) metabolizing enzyme GSNO reductase. In $GSNOR^{-/-}$ mice, GSNO turnover is required not only for preventing the accumulation of SNO that predisposes to cardiovascular diseases, but also for regulating SNO turnover in the context of physiological signaling especially important for regulation of blood pressure and vascular homeostasis (Lima et al., 2010; Liu et al., 2004) as well as angiogenesis (Lima et al., 2009).

S-nitrosylation is a redox-sensitive and reversible *post*-translational modification on proteins, providing an important mechanism for regulating the activity of various proteins in most biological pathways (Hess et al., 2005). Over two hundred proteins have been found to be nitrosylated *in vivo*, consistent with the ubiquity of regulatory and/or active-site thiols across protein classes (Hess et al., 2005). Functional studies have demonstrated that SNO leads to decreased activity of most enzymes, such as cytochrome c oxidase (Zhang et al., 2005), creatine kinase (Arstall et al., 1998), Ca^{2+}/calmodulin-dependent protein kinases (Takata et al., 2011), protein tyrosine phosphatases (Xian et al., 2000), caspase-3 (Maejima et al., 2005), hypoxia-inducible factors (Li et al., 2007), eNOS (Ravi et al., 2004), and NADPH oxidase (Selemidis et al., 2007), but also increases the activity of α-ketoglutarate dehydrogenase (Sun et al., 2007) and cyclooxygenase-2 (Atar et al., 2006).

Because the direct protein targets affected by NO in UAEC and whether this plays a role in UBF regulation by estrogen and pregnancy have never been investigated, differential display of the *nitroso*-proteomes in resting and estrogen-treated UAEC will provide abundant first-hand information to these ends. We therefore used the powerful CyDye switch/2D-DIGE proteomics method as described in our recent report (Zhang et al., 2010) to analyze the estrogen-responsive *nitroso*-proteomes in UAEC. We observed numerous *SNO*-proteins on the 2D-DIGE gel. According to their visibility and estrogen-responsiveness we have focused our attention on 60 spots, of which 54 were positively identified and 32 were significantly enhanced by E2 stimulation. Similar to recent reports in cardiomyocytes (Lin et al., 2009) and HUVEC (Zhang et al., 2010), E2 acutely decreased the levels of some other *SNO*-proteins. Protein "*de*-nitrosylation" by estrogen stimulation in ECs is very intriguing and was quite unexpected. This is because within the time frame tested estrogens stimulate endothelial NO production (Chen et al., 2004; Haynes et al., 2000), which presumptively leads to enhanced SNO in ECs. Although the underlying mechanism is elusive, this is likely linked to "*trans*-nitrosylation" by which these *SNO*-proteins may denote their NO moiety for nitrosylating other proteins. Other scenarios for estrogen-induced "*de*-nitrosylation" might be due to changes in the activity of the enzymes important for "*trans*- or *de*-" nitrosylation, such as GSNO reductase (Liu et al., 2001) and thioredoxin reductase (Benhar et al., 2008), that in turn regulate dynamic protein SNO. These ideas are critical for delineating the mechanism underlying estrogen regulation of SNO and waiting for further investigations.

It is noteworthy that different spots on 2D-DIGE may be the same protein. For example, spots 2 and 53 have been identified as cofilin-1; however, each responded differently in SNO to E2 stimulation. SNO of spot 2 is significantly increased by 2.47 fold, while spot 53 was significantly decreased 70% by E2. Similar scenarios also apply to annexin A2 (spots 13&43), pyruvate kinase (spots 18&36&37), phosphoglycerate mutase 1 (spots 27&47), and triosephosphate isomerase 1 (spots 7&9&39). The position shift of proteins on 2D-DIGE is specifically due to a change in isoelectric point (PI) as a result of various posttranslational modifications. Thus, these data illustrate that SNO of the same protein with different PI responds to E2 stimulation differently, demonstrating that protein *post*-translational modifications may lead to different responses in SNO to stimulation by estrogens. Also of note is that the powerful Cydye Switch/2DIGE MS for proteomics analysis of *SNO*-proteins is also capable for identifying specific SNO site in proteins. Further analysis by MS/MS and the MASCOT algorithm of the trypsin-digested peptides of GAPDH subjected from Cydye Switch showed that the CyDye binding site was Cys139, which was identical to a previous report (Paige et al., 2008).

The partial cellular *nitroso*-proteomes identified in UAEC contains some of the same *SNO*-proteins that we have recently identified in HUVEC (Zhang et al., 2010), including peroxiredoxins, annexin, cofilin-1, enolase1, glutathione transferases, ubiquitin and proteasome, triosephosphate isomerase, transketolase, eukaryotic translation elongation

factor 1 gamma, eukaryotic translation elongation factor 2. Identification of these *SNO*-proteins in both UAEC and HUVEC demonstrates that SNO regulates some common functions in both endothelial cells derived from maternal artery and fetal vein, respectively. Among the partial endothelial *nitroso*-proteomes in UAEC, we found a sub-class of proteins known to be important in cytoskeleton regulation, like vimentin, spectirn, fascin and cofilin-1. Of particular note, cofilin-1 is a member of small (15-20 kDa) actin-binding protein family essential for actin remodeling via severing and nucleating actin filaments (Bamburg and Wiggan, 2002). A recent study suggested a possible role of cysteine modification in cofilin-1 function (Klamt et al., 2009). Of interest, *SNO*-cofilin-1 is a highly estrogen-responsive protein in the *nitroso*-proteome in UAEC (current study) and HUVEC (Zhang et al., 2010). We have recently observed that SNO results in enhanced actin severing activity of cofilin-1 and further initiates cytoskeleton reorganization and endothelial cell migration (Zhang and Chen, unpublished data). This pathway may also partly account for the E2 induced UAEC angiogenic processes seen in these cells that occur solely via ERβ activation (Jobe et al., 2010).

We have identified several *SNO*-proteins in UAEC that have never been reported to date. For example, aconitase II is an enzyme that catalyses the stereo-specific isomerization of citrate to isocitrate via cis-aconitate in the tricarboxylic acid cycle, a non-redox-active process (Beinert et al., 1996). Exposure of aconitase to a NO donor resulted in loss of its enzyme activity (Kennedy et al., 1997). Aldehyde reductase is primarily known for catalyzing the reduction of glucose to sorbitol, the first step in polyol pathway of glucose metabolism (Petrash, 2004). Pyruvate kinase is an enzyme also involved in glycolysis (Liapounova et al., 2006). Citrate synthase exists in nearly all living cells and stands as a pace-making enzyme in the first step of the citric acid cycle (Wiegand and Remington, 1986). Superoxide dismutase 2 transforms toxic superoxide to water (Muller et al., 2007). Zyxin is a zinc-binding phosphoprotein that concentrates at focal adhesions and along the actin cytoskeleton and is thought to modulate the cytoskeletal organization of actin bundles (Macalma et al., 1996). Fascin binds beta-catenin and colocalizes at the leading edges and borders, regulating cytoskeletal structures for the maintenance of cell adhesion, coordinating motility and invasion (Adams, 2004). Hypoxia up-regulated protein 1 plays an important role in protein folding and secretion in the endoplasmic reticulum (Ikeda et al., 1997). Even though these proteins play important roles in cellular functions, the complete consequence of SNO on their functions have yet to be determined.

What are the physiological significances of estrogen stimulation of SNO in UAEC as to whether this relates to UBF biology and pregnancy? Normal pregnancy is associated with dramatic rises in UBF (partly indicative of vasodilatation) that provide oxygen and nutrient supplies instrumental for fetal/placental development. Insufficient elevations in UBF result in a deficit of oxygen and nutrient supplied, which further causes fetal intrauterine growth restriction and higher prenatal and neonatal morbidity or even mortality (Lang et al., 2003). Concomitantly, levels of circulating estrogens increase substantially, exemplified by more than 1000-fold greater levels of total plasma estrogens in the third trimester pregnant compared to nonpregnant women (Albrecht and Pepe, 1990). These data implicate an important role of estrogens for normal pregnancy by upregulating UBF, which is directly supported by animal and human studies showing rapid and dramatic uterine and systemic vasodilatation following estrogen administration (Magness and Rosenfeld, 1989; Volterrani et al., 1995). It is evident that the most reasonable biological pathway that partly underlies estrogen-induced uterine vasodilatation and rises in UBF is enhanced endothelial NO production via rapid activation (Chen et al., 2004) or latent expression of eNOS protein in UAEC (Chen et al., 2006; Rupnow et al 2001; Vagnoni et al., 1998). Despite extensive studies showing a critical role of NO in estrogen-induced and pregnancy-associated uterine vasodilatation, surprisingly, the direct targets of NO itself in UAEC have not yet

determined. SNO represents a major pathway for NO to directly control the functions of a plethora of proteins that regulate nearly all major biological pathways (Derakhshan et al., 2007; Hess et al., 2005; Lane et al., 2001). Our current findings clearly demonstrate that estrogen stimulates dynamic SNO of a plethora of proteins in UAEC that are linked to endogenous NO production via eNOS and mostly ERβ that is possibly located on the plasma membrane. Pathway analysis of the *SNO*-proteins identified in the resting and estrogen-treated UAEC revealed that protein SNO regulates diverse biological functions. Thus, the present studies implicate that SNO may offer a novel mechanism that estrogens utilize to regulate uterine vasodilatation.

Supplementary Material

Refer to Web version on PubMed Central for supplementary material.

Acknowledgments

We greatly appreciate Dr. Mark J. Evans for kindly providing the replication-defective adenoviruses carrying full length wild-type human ERα and ERβ for our studies.

Sources of Funding: This work was supported in part by National Institutes of Health Grants R21 HL98746, RO1 HL70562 and HL74947 (to D-B.C) and RO1 HL49210, PO1 HD38843, RO1 HL87144 (to RRM).

References

Adams JC. Roles of fascin in cell adhesion and motility. Curr Opin Cell Biol. 2004; 16(5):590–596. [PubMed: 15363811]

Albrecht ED, Pepe GJ. Placental steroid hormone biosynthesis in primate pregnancy. Endocr Rev. 1990; 11(1):124–150. [PubMed: 2180685]

Arstall MA, Bailey C, Gross WL, Bak M, Balligand JL, Kelly RA. Reversible S-nitrosation of creatine kinase by nitric oxide in adult rat ventricular myocytes. J Mol Cell Cardiol. 1998; 30(5):979–988. [PubMed: 9618238]

Atar S, Ye Y, Lin Y, Freeberg SY, Nishi SP, Rosanio S, Huang MH, Uretsky BF, Perez-Polo JR, Birnbaum Y. Atorvastatin-induced cardioprotection is mediated by increasing inducible nitric oxide synthase and consequent S-nitrosylation of cyclooxygenase-2. Am J Physiol Heart Circ Physiol. 2006; 290(5):H1960–1968. [PubMed: 16339820]

Bamburg JR, Wiggan OP. ADF/cofilin and actin dynamics in disease. Trends Cell Biol. 2002; 12(12): 598–605. [PubMed: 12495849]

Beinert H, Kennedy MC, Stout CD. Aconitase as Ironminus signSulfur Protein, Enzyme, and Iron-Regulatory Protein. Chem Rev. 1996; 96(7):2335–2374. [PubMed: 11848830]

Benhar M, Forrester MT, Hess DT, Stamler JS. Regulated protein denitrosylation by cytosolic and mitochondrial thioredoxins. Science. 2008; 320(5879):1050–1054. [PubMed: 18497292]

Bird IM, Sullivan JA, Di T, Cale JM, Zhang L, Zheng J, Magness RR. Pregnancy-dependent changes in cell signaling underlie changes in differential control of vasodilator production in uterine artery endothelial cells. Endocrinology. 2000; 141(3):1107–1117. [PubMed: 10698187]

Byers MJ, Zangl A, Phernetton TM, Lopez G, Chen DB, Magness RR. Endothelial vasodilator production by ovine uterine and systemic arteries: ovarian steroid and pregnancy control of ERalpha and ERbeta levels. J Physiol. 2005; 565(Pt 1):85–99. [PubMed: 15774511]

Chakrabarti S, Lekontseva O, Peters A, Davidge ST. 17beta-Estradiol induces protein S-nitrosylation in the endothelium. Cardiovasc Res. 2010; 85(4):796–805. [PubMed: 19914929]

Chen DB, Bird IM, Zheng J, Magness RR. Membrane estrogen receptor-dependent extracellular signal-regulated kinase pathway mediates acute activation of endothelial nitric oxide synthase by estrogen in uterine artery endothelial cells. Endocrinology. 2004; 145(1):113–125. [PubMed: 14512434]

Chen DB, Jia S, King AG, Barker A, Li SM, Mata-Greenwood E, Zheng J, Magness RR. Global protein expression profiling underlines reciprocal regulation of caveolin 1 and endothelial nitric

oxide synthase expression in ovariectomized sheep uterine artery by estrogen/progesterone replacement therapy. Biol Reprod. 2006; 74(5):832–838. [PubMed: 16436525]

Derakhshan B, Hao G, Gross SS. Balancing reactivity against selectivity: the evolution of protein S-nitrosylation as an effector of cell signaling by nitric oxide. Cardiovasc Res. 2007; 75(2):210–219. [PubMed: 17524376]

Evans MJ, Harris HA, Miller CP, Karathanasis SK, Adelman SJ. Estrogen receptors alpha and beta have similar activities in multiple endothelial cell pathways. Endocrinology. 2002; 143(10):3785–3795. [PubMed: 12239089]

Ford SP. Control of uterine and ovarian blood flow throughout the estrous cycle and pregnancy of ewes, sows and cows. J Anim Sci. 1982; 55 2:32–42. [PubMed: 6765316]

Forstermann U, Boissel JP, Kleinert H. Expressional control of the 'constitutive' isoforms of nitric oxide synthase (NOS I and NOS III). Faseb J. 1998; 12(10):773–790. [PubMed: 9657518]

Gibson TC, Phernetton TM, Wiltbank MC, Magness RR. Development and use of an ovarian synchronization model to study the effects of endogenous estrogen and nitric oxide on uterine blood flow during ovarian cycles in sheep. Biol Reprod. 2004; 70(6):1886–1894. [PubMed: 14985241]

Hara MR, Agrawal N, Kim SF, Cascio MB, Fujimuro M, Ozeki Y, Takahashi M, Cheah JH, Tankou SK, Hester LD, Ferris CD, Hayward SD, Snyder SH, Sawa A. S-nitrosylated GAPDH initiates apoptotic cell death by nuclear translocation following Siah1 binding. Nat Cell Biol. 2005; 7(7):665–674. [PubMed: 15951807]

Haynes MP, Sinha D, Russell KS, Collinge M, Fulton D, Morales-Ruiz M, Sessa WC, Bender JR. Membrane estrogen receptor engagement activates endothelial nitric oxide synthase via the PI3-kinase-Akt pathway in human endothelial cells. Circ Res. 2000; 87(8):677–682. [PubMed: 11029403]

Hess DT, Matsumoto A, Kim SO, Marshall HE, Stamler JS. Protein S-nitrosylation: purview and parameters. Nat Rev Mol Cell Biol. 2005; 6(2):150–166. [PubMed: 15688001]

Ikeda J, Kaneda S, Kuwabara K, Ogawa S, Kobayashi T, Matsumoto M, Yura T, Yanagi H. Cloning and expression of cDNA encoding the human 150 kDa oxygen-regulated protein, ORP150. Biochem Biophys Res Commun. 1997; 230(1):94–99. [PubMed: 9020069]

Jaffrey SR, Snyder SH. The biotin switch method for the detection of S-nitrosylated proteins. Sci STKE. 2001; 2001(86):PL1. [PubMed: 11752655]

Jobe SO, Ramadoss J, Koch JM, Jiang Y, Zheng J, Magness RR. Estradiol-17beta and its cytochrome P450- and catechol-O-methyltransferase-derived metabolites stimulate proliferation in uterine artery endothelial cells: role of estrogen receptor-alpha versus estrogen receptor-beta. Hypertension. 2010; 55(4):1005–1011. [PubMed: 20212268]

Kang-Decker N, Cao S, Chatterjee S, Yao J, Egan LJ, Semela D, Mukhopadhyay D, Shah V. Nitric oxide promotes endothelial cell survival signaling through S-nitrosylation and activation of dynamin-2. J Cell Sci. 2007; 120(Pt 3):492–501. [PubMed: 17251380]

Kennedy MC, Antholine WE, Beinert H. An EPR investigation of the products of the reaction of cytosolic and mitochondrial aconitases with nitric oxide. J Biol Chem. 1997; 272(33):20340–20347. [PubMed: 9252338]

Klamt F, Zdanov S, Levine RL, Pariser A, Zhang Y, Zhang B, Yu LR, Veenstra TD, Shacter E. Oxidant-induced apoptosis is mediated by oxidation of the actin-regulatory protein cofilin. Nat Cell Biol. 2009; 11(10):1241–1246. [PubMed: 19734890]

Lane P, Hao G, Gross SS. S-nitrosylation is emerging as a specific and fundamental posttranslational protein modification: head-to-head comparison with O-phosphorylation. Sci STKE. 2001; 2001(86):RE1. [PubMed: 11752656]

Lang U, Baker RS, Braems G, Zygmunt M, Kunzel W, Clark KE. Uterine blood flow--a determinant of fetal growth. Eur J Obstet Gynecol Reprod Biol. 2003; 110 1:S55–61. [PubMed: 12965091]

Li F, Sonveaux P, Rabbani ZN, Liu S, Yan B, Huang Q, Vujaskovic Z, Dewhirst MW, Li CY. Regulation of HIF-1alpha stability through S-nitrosylation. Mol Cell. 2007; 26(1):63–74. [PubMed: 17434127]

Liao WX, Feng L, Zhang H, Zheng J, Moore TR, Chen DB. Compartmentalizing VEGF-induced ERK2/1 signaling in Placental Artery Endothelial Cell Caveolae: a Paradoxical Role of Caveolin-1 in Placental Angiogenesis in vitro. Mol Endocrinol. 2009; 23:1428–1444. [PubMed: 19477952]

Liao WX, Magness RR, Chen DB. Expression of estrogen receptors-alpha and -beta in the pregnant ovine uterine artery endothelial cells in vivo and in vitro. Biol Reprod. 2005; 72(3):530–537. [PubMed: 15564597]

Liapounova NA, Hampl V, Gordon PM, Sensen CW, Gedamu L, Dacks JB. Reconstructing the mosaic glycolytic pathway of the anaerobic eukaryote Monocercomonoides. Eukaryot Cell. 2006; 5(12): 2138–2146. [PubMed: 17071828]

Lima B, Forrester MT, Hess DT, Stamler JS. S-nitrosylation in cardiovascular signaling. Circ Res. 2010; 106(4):633–646. [PubMed: 20203313]

Lima B, Lam GK, Xie L, Diesen DL, Villamizar N, Nienaber J, Messina E, Bowles D, Kontos CD, Hare JM, Stamler JS, Rockman HA. Endogenous S-nitrosothiols protect against myocardial injury. Proc Natl Acad Sci U S A. 2009; 106(15):6297–6302. [PubMed: 19325130]

Lin J, Steenbergen C, Murphy E, Sun J. Estrogen receptor-beta activation results in S-nitrosylation of proteins involved in cardioprotection. Circulation. 2009; 120(3):245–254. [PubMed: 19581491]

Liu L, Hausladen A, Zeng M, Que L, Heitman J, Stamler JS. A metabolic enzyme for S-nitrosothiol conserved from bacteria to humans. Nature. 2001; 410(6827):490–494. [PubMed: 11260719]

Liu L, Yan Y, Zeng M, Zhang J, Hanes MA, Ahearn G, McMahon TJ, Dickfeld T, Marshall HE, Que LG, Stamler JS. Essential roles of S-nitrosothiols in vascular homeostasis and endotoxic shock. Cell. 2004; 116(4):617–628. [PubMed: 14980227]

Macalma T, Otte J, Hensler ME, Bockholt SM, Louis HA, Kalff-Suske M, Grzeschik KH, von der Ahe D, Beckerle MC. Molecular characterization of human zyxin. J Biol Chem. 1996; 271(49):31470–31478. [PubMed: 8940160]

Maejima Y, Adachi S, Morikawa K, Ito H, Isobe M. Nitric oxide inhibits myocardial apoptosis by preventing caspase-3 activity via S-nitrosylation. J Mol Cell Cardiol. 2005; 38(1):163–174. [PubMed: 15623433]

Magness RR, Phernetton TM, Gibson TC, Chen DB. Uterine blood flow responses to ICI 182 780 in ovariectomized oestradiol-17beta-treated, intact follicular and pregnant sheep. J Physiol. 2005; 565(Pt 1):71–83. [PubMed: 15774510]

Magness RR, Rosenfeld CR. Local and systemic estradiol-17 beta: effects on uterine and systemic vasodilation. Am J Physiol. 1989; 256(4 Pt 1):E536–542. [PubMed: 2650565]

Magness RR, Shaw CE, Phernetton TM, Zheng J, Bird IM. Endothelial vasodilator production by uterine and systemic arteries. II. Pregnancy effects on NO synthase expression. Am J Physiol. 1997; 272(4 Pt 2):H1730–1740. [PubMed: 9139957]

Magness RR, Sullivan JA, Li Y, Phernetton TM, Bird IM. Endothelial vasodilator production by uterine and systemic arteries. VI. Ovarian and pregnancy effects on eNOS and NO(x). Am J Physiol Heart Circ Physiol. 2001; 280(4):H1692–1698. [PubMed: 11247781]

Markee JE. Rhythmic vascular uterine changes. Am J Physiol. 1932; 100:32–39.

Muller FL, Lustgarten MS, Jang Y, Richardson A, Van Remmen H. Trends in oxidative aging theories. Free Radic Biol Med. 2007; 43(4):477–503. [PubMed: 17640558]

Murad F. Cyclic guanosine monophosphate as a mediator of vasodilation. J Clin Invest. 1986; 78(1):1–5. [PubMed: 2873150]

Paige JS, Xu G, Stancevic B, Jaffrey SR. Nitrosothiol reactivity profiling identifies S-nitrosylated proteins with unexpected stability. Chem Biol. 2008; 15(12):1307–1316. [PubMed: 19101475]

Petrash JM. All in the family: aldose reductase and closely related aldo-keto reductases. Cell Mol Life Sci. 2004; 61(7-8):737–749. [PubMed: 15094999]

Radi R, Peluffo G, Alvarez MN, Naviliat M, Cayota A. Unraveling peroxynitrite formation in biological systems. Free Radic Biol Med. 2001; 30(5):463–488. [PubMed: 11182518]

Ravi K, Brennan LA, Levic S, Ross PA, Black SM. S-nitrosylation of endothelial nitric oxide synthase is associated with monomerization and decreased enzyme activity. Proc Natl Acad Sci U S A. 2004; 101(8):2619–2624. [PubMed: 14983058]

Rosenfeld CR, Cox BE, Roy T, Magness RR. Nitric oxide contributes to estrogen-induced vasodilation of the ovine uterine circulation. J Clin Invest. 1996; 98(9):2158–2166. [PubMed: 8903336]

Rupnow HL, Phernetton TM, Shaw CE, Modrick ML, Bird IM, Magness RR. Endothelial vasodilator production by uterine and systemic arteries. VII. Estrogen and progesterone effects on eNOS. Am J Physiol Heart Circ Physiol. 2001; 280(4):H1699–1705. [PubMed: 11247782]

Selemidis S, Dusting GJ, Peshavariya H, Kemp-Harper BK, Drummond GR. Nitric oxide suppresses NADPH oxidase-dependent superoxide production by S-nitrosylation in human endothelial cells. Cardiovasc Res. 2007; 75(2):349–358. [PubMed: 17568572]

Sirover MA. New insights into an old protein: the functional diversity of mammalian glyceraldehyde-3-phosphate dehydrogenase. Biochim Biophys Acta. 1999; 1432(2):159–184. [PubMed: 10407139]

Smith KM, Moore LC, Layton HE. Advective transport of nitric oxide in a mathematical model of the afferent arteriole. Am J Physiol Renal Physiol. 2003; 284(5):F1080–1096. [PubMed: 12712988]

Stamler JS, Jaraki O, Osborne J, Simon DI, Keaney J, Vita J, Singel D, Valeri CR, Loscalzo J. Nitric oxide circulates in mammalian plasma primarily as an S-nitroso adduct of serum albumin. Proc Natl Acad Sci U S A. 1992a; 89(16):7674–7677. [PubMed: 1502182]

Stamler JS, Simon DI, Osborne JA, Mullins ME, Jaraki O, Michel T, Singel DJ, Loscalzo J. S-nitrosylation of proteins with nitric oxide: synthesis and characterization of biologically active compounds. Proc Natl Acad Sci U S A. 1992b; 89(1):444–448. [PubMed: 1346070]

Sun J, Morgan M, Shen RF, Steenbergen C, Murphy E. Preconditioning results in S-nitrosylation of proteins involved in regulation of mitochondrial energetics and calcium transport. Circ Res. 2007; 101(11):1155–1163. [PubMed: 17916778]

Takata T, Kimura J, Tsuchiya Y, Naito Y, Watanabe Y. Calcium/calmodulin-dependent protein kinases as potential targets of nitric oxide. Nitric Oxide. 2011

Truss M, Beato M. Steroid hormone receptors: interaction with deoxyribonucleic acid and transcription factors. Endocr Rev. 1993; 14(4):459–479. [PubMed: 8223341]

Vagnoni KE, Shaw CE, Phernetton TM, Meglin BM, Bird IM, Magness RR. Endothelial vasodilator production by uterine and systemic arteries. III. Ovarian and estrogen effects on NO synthase. Am J Physiol. 1998; 275(5 Pt 2):H1845–1856. [PubMed: 9815093]

Volterrani M, Rosano G, Coats A, Beale C, Collins P. Estrogen acutely increases peripheral blood flow in postmenopausal women. Am J Med. 1995; 99(2):119–122. [PubMed: 7625415]

Wanstall JC, Homer KL, Doggrell SA. Evidence for, and importance of, cGMP-independent mechanisms with NO and NO donors on blood vessels and platelets. Curr Vasc Pharmacol. 2005; 3(1):41–53. [PubMed: 15638781]

Wiegand G, Remington SJ. Citrate synthase: structure, control, and mechanism. Annu Rev Biophys Biophys Chem. 1986; 15:97–117. [PubMed: 3013232]

Xian M, Wang K, Chen X, Hou Y, McGill A, Zhou B, Zhang ZY, Cheng JP, Wang PG. Inhibition of protein tyrosine phosphatases by low-molecular-weight S-nitrosothiols and S-nitrosylated human serum albumin. Biochem Biophys Res Commun. 2000; 268(2):310–314. [PubMed: 10679200]

Zhang HH, Feng L, Livnat I, Hoh JK, Shim JY, Liao WX, Chen DB. Estradiol-17β stimulates specific receptor and endogenous nitric oxide-dependent dynamic endothelial protein S-nitrosylation: analysis of endothelial nitrosyl-proteome. Endocrinology. 2010; 151(8):3874–3887. [PubMed: 20519370]

Zhang HH, Wang YP, Chen DB. Analysis of Nitroso-Proteomes in normotensive and severe preeclamptic human placentas. Biol Reprod. 2011

Zhang J, Jin B, Li L, Block ER, Patel JM. Nitric oxide-induced persistent inhibition and nitrosylation of active site cysteine residues of mitochondrial cytochrome-c oxidase in lung endothelial cells. Am J Physiol Cell Physiol. 2005; 288(4):C840–849. [PubMed: 15561762]

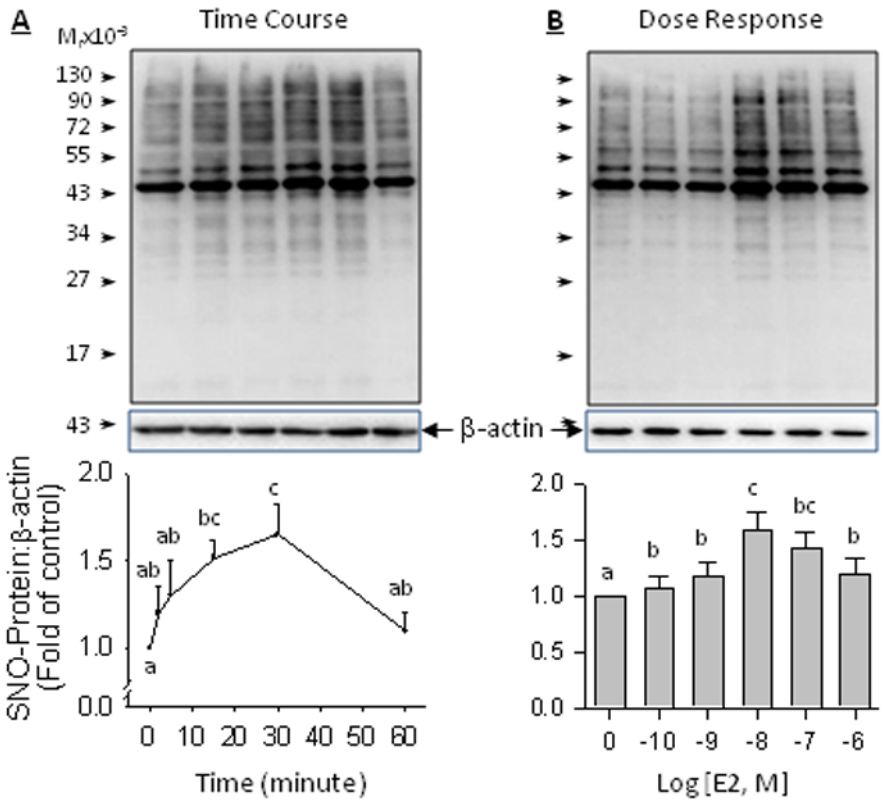

Fig. 1. Effects of estradiol-17β (E2) on total *SNO*-protein profiles in ovine uterine artery endothelial cells (UAEC) on SDS-PAGE: time courses and Dose-responses

Subconfluent UAEC were treated with or without 10 nM E2 for the indicated times (up to 1h, A) or with increasing concentration of E2 (0.1 nM to 1 μM, B) for 30 minutes. Total protein extracts were harvested and subjected to biotin-switch reaction. The biotin-labeled *SNO*-proteins were analyzed by 10% SDS-PAGE and detected by Western blot with an anti-biotin antibody. Representative blots of *SNO*-proteins and β-actin (loading control) of one typical experiment are shown. Lower graphs summarize data (mean ± SEM, n =3) from three independent experiments using UAEC from different pregnant ewes. Bars with different letters differ significantly.

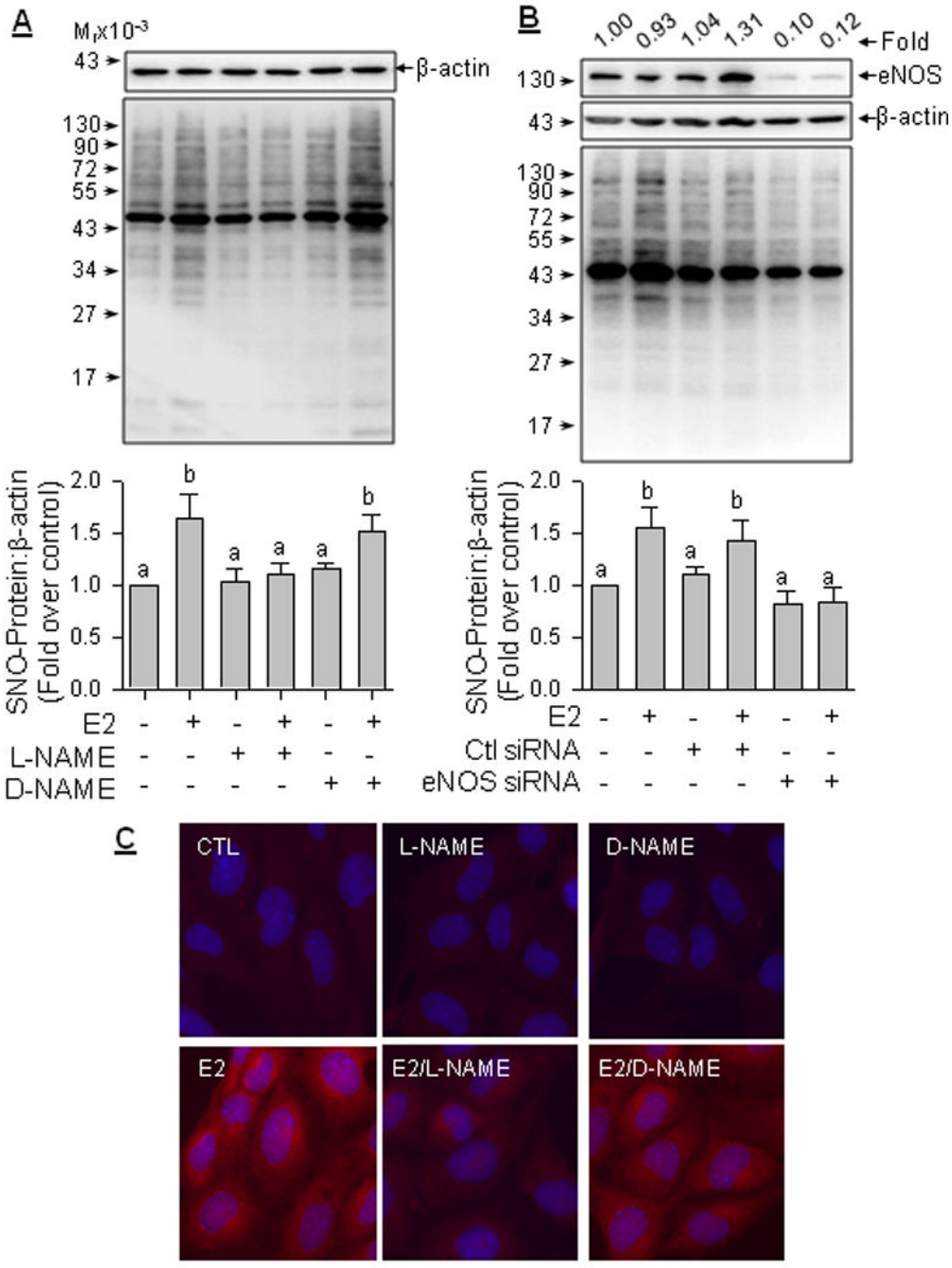

Fig. 2. Effect of nitric oxide synthase inhibition on E2-induced SNO in ovine uterine artery endothelial cells (UAEC)

UAEC were pretreated with or without L-NAME or D-NAME (1 mM) for 1 h, then treated with or without E2 (10 nM) for 30 min. A: *SNO*-proteins were detected by the biotin-switch method. Representative blots of *SNO*-proteins and β-actin of one typical experiment are shown. Lower graphs summarize data (mean ± SEM, n =3) from three independent experiments using UAEC from different pregnant ewes. B: Effect of knockdown of endothelial nitric oxide synthase by specific siRNA on E2-induced SNO. UAEC transfected with or without scramble control siRNA or eNOS siRNA were treated with or without E2 (10 nM) for 30 min. *SNO*-proteins were detected by the biotin-switch method.

Representative blots of *SNO*-proteins, eNOS and β-actin of one typical experiment are shown. Lower graphs summarized data (mean ± SEM, n =3) from three independent experiments using UAEC from different pregnant ewes. CTL: control. Bars with different letters differ significantly. C: *SNO*-proteins were detected in intact cells by a modified BST using MTSEA-Texas Red as the labeling reagent. Nuclei were labeled by DAPI (blue). Fluorescence micrographs (200×) shown depict one of four separate experiments using cells from different pregnant ewes.

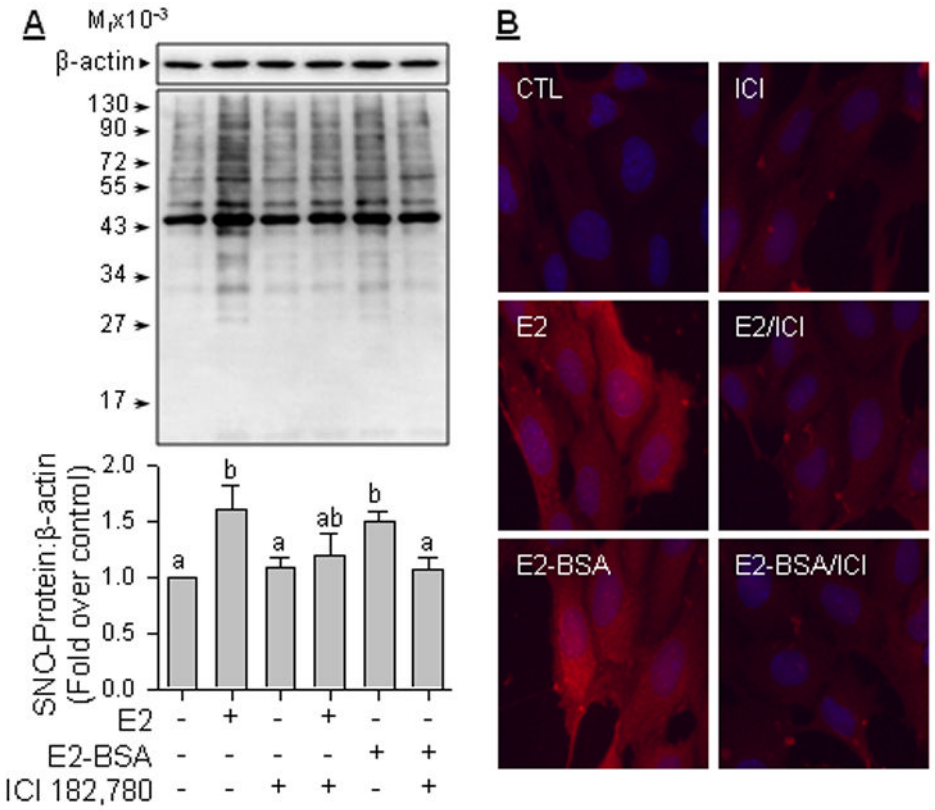

Fig. 3. Effects of ICI 182,780 on E2-induced SNO in ovine uterine artery endothelial cells (UAEC)

UAEC were pretreated with or without ICI 182,780 (1 μM) for 1h, then treated with or without 10 nM of E2 or E2-BSA for 30 min. A: *SNO*-proteins were detected by the Biotin-switch method. Representative blots of *SNO*-proteins and β-actin of one typical experiment are shown. Lower graphs summarize data (mean ± SEM, n =3) from three independent experiments using UAEC from different pregnant ewes. Bars with different letters differ significantly. B: *SNO*-proteins were detected in intact cells by a modified BST using MTSEA-Texas Red as the labeling reagent. Nuclei were labeled by DAPI (blue). Fluorescence micrographs (200 ×) shown depict one of three separate experiments using cells from different pregnant ewes.

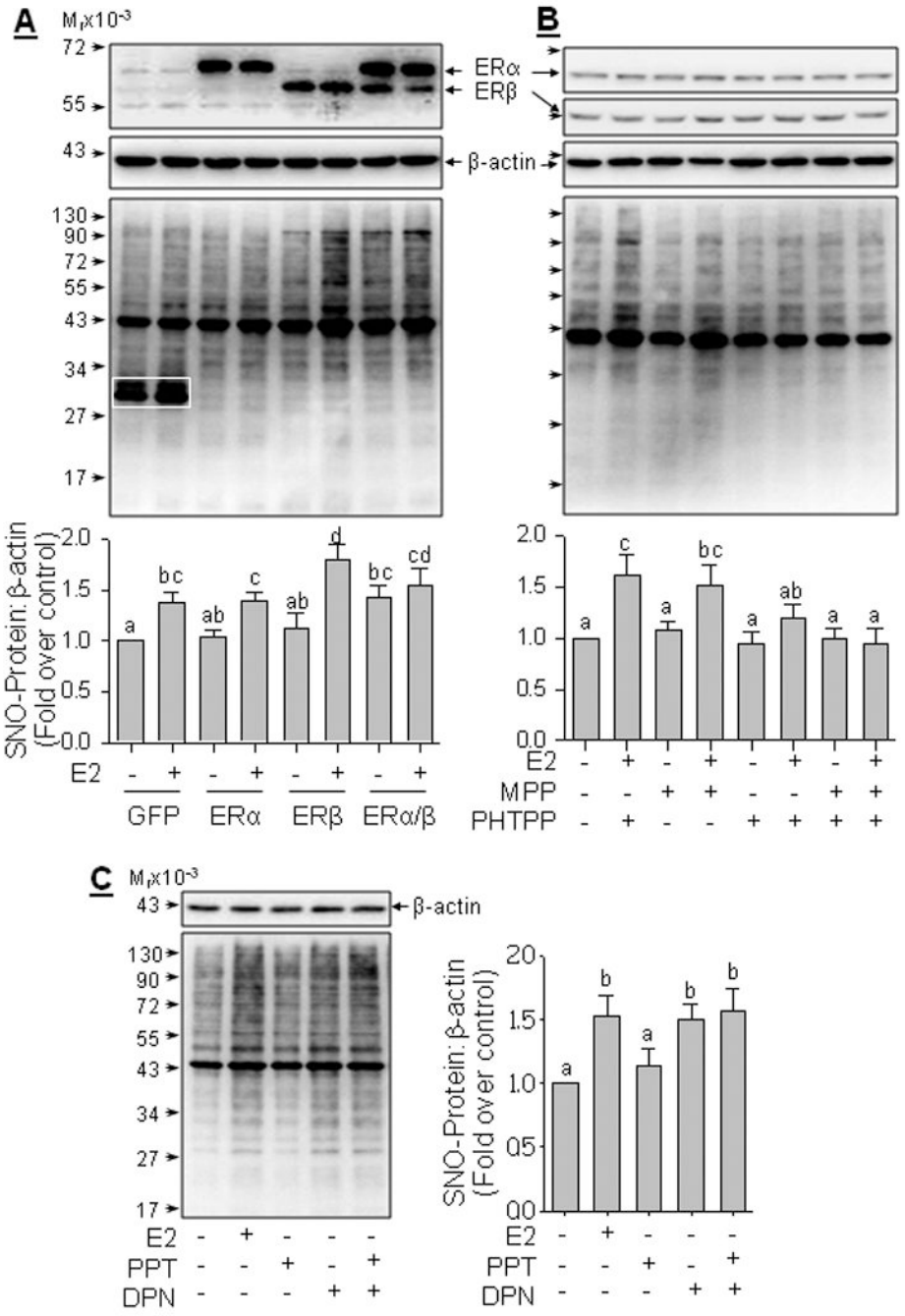

Fig. 4. Specific Roles of ERα and ERβ in E2-induced SNO in ovine uterine artery endothelial cells (UAEC)

A: UAEC infected with Ad-GFP or Ad-ERα, Ad-ERβ, or both were treated with or without E2 (10 nM, 30 min). B: UAEC were pretreated with or without the selective antagonist (1 μM) of ERα (MPP), ERβ (PHTPP), or their combination for 60 min, followed by E2 treatment (10 nM, 30 min). C: UAEC were treated with 10 nM of specific agonists of ERα (PPT), or ERβ (DPN), or both for 30 min. *SNO*-proteins were detected by the biotin-switch method. Representative blots of *SNO*-proteins and β-actin of one typical experiment are shown. β-actin was used as a loading control. Bar graphs summarize data (mean ± SEM, n

=3) from three independent experiments using UAEC from different pregnant ewes. Bars with different letters differ significantly.

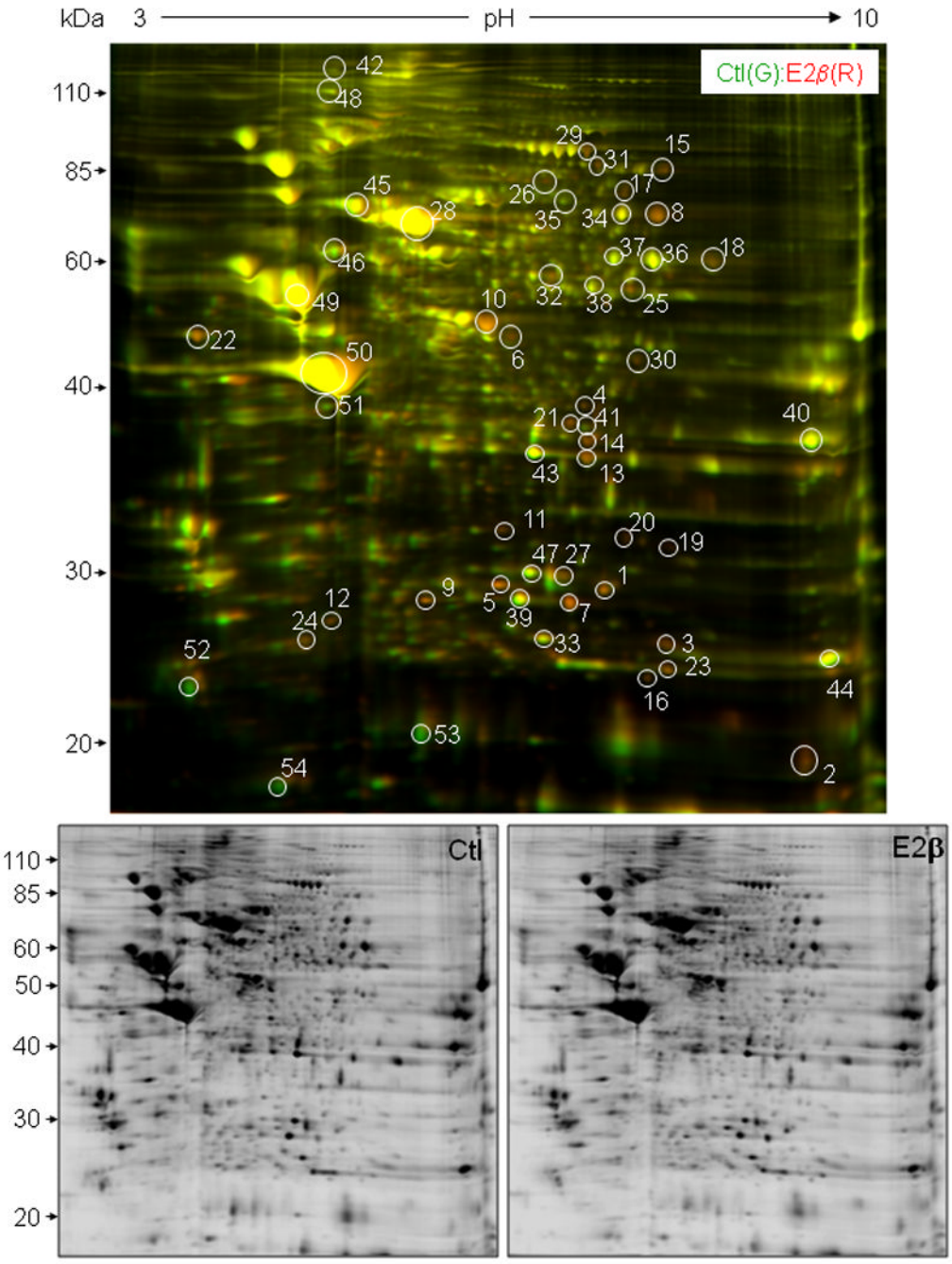

Fig. 5. CyDye switch, two dimensional fluorescence difference gel electrophoresis (2D-DIGE) analysis of *nitroso*-proteomes in control and estrogen treated ovine uterine artery endothelial cells (UAEC)

UAEC were treated with or without E2 (10 nM) for 30 minutes. Total cell extracts (50 μg protein/treatment) were incubated with ascorbate. Control samples were labeled with Cy3 (green) and E2-treated samples were labeled with Cy5 (Red). The samples were then mixed (total 100 μg protein) and then separated on analytical 2-D DIGE. The gel was scanned with a fluorescence scanner in green (Cy3, 548/560nm) and red (Cy5, 641/660nm) channels. A merged fluorescence image shown represents one of three separate experiments using cells from different placentas. Red, green and yellow spots represent *SNO*-proteins that were

increased, decreased or unchanged by E2, respectively. The spots circled and numbered represent 54 *SNO*-proteins as listed in table 1, which were successfully identified by matrix-assisted laser desorption ionization/time of flight and tandem mass spectrometry. The lower black and white images shown represent fluorescent signals obtained from the red and green channels of one of three experiments using UAEC from different pregnant ewes.

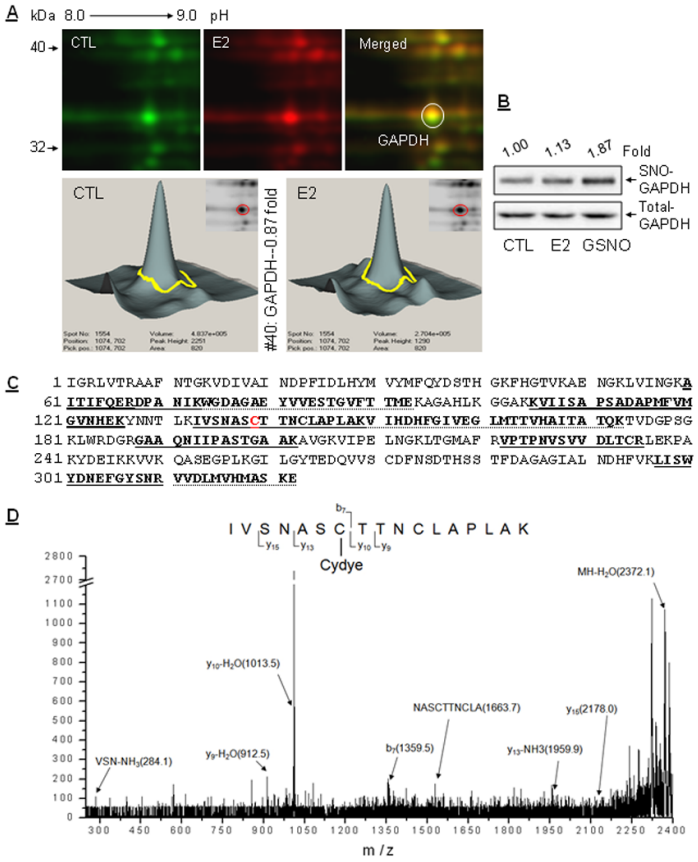

Fig. 6. SNO of Glyceraldehyde 3-phosphate dehydrogenase (GADPH) in E2 treated ovine uterine artery endothelial cells (UAEC) and identification of its Cydye binding site

(A) Spot identified as GAPDH was shown in a small area (32-40kDa and pH8.0-9.0) of the CyDdye switch/2D-DIGE gel as shown in Fig. 5 with images of Cy3 labeled control (green, up panel left) and Cy5 labeled E2-treated (red, up panel middle) samples and their merged one (up panel right). ImageQuant software was used to generate the 3D-images (lower panel) in control and E2-treated cells. (B) Whole cell lysates of UAEC treated with E2, GSNO, or vehicle were prepared and subjected to Biotin Switch/Avidin caputure. Total and *SNO*-GAPDH levels were determined by immumoblotting with anti-GAPDH antibody. Fold changes compared to control were listed on each lane. (C, D) Cydye labeled GAPDH spots were picked up from the 2D-DIGE gel, subjected to trypsin digestion and MALDI-TOF MS, then searched with the NCBI non-redundant *Bos Taurus* and *Ovis aries* amino acid sequence databases. The trypsinized peptides with CyDye-bound cysteines were analysed by comparing tandom MS/MS spetra with a monoisotopic mass shift (672.2981 Dalton for Cy3 or 684.2981 Dalton for Cy5). The identified peptides of GAPDH were labeled by underlines and *SNO*-cysteine is labeled in red in the full amino acid sequence of ovine GAPDH. The MS/MS analysis of CyDye-bound peptide is shown as a peak list.

Table 1

The *nitroso*-proteomes in resting and estradiol-17β-treated uterine artery endothelial cells identified by Cydye switch and 2 two-dimensional fluorescence difference gel electrophoresis and matrix assisted laser desorption/ionization-time of flight (MALDI-TOF)/tandam mass spectrometry.

Spot #., Protein Name	GeneID	MW (Da) / PI	# Pep Matched	Protein Score	Ratio (E2/Ctl)	P-value[1]
					Mean ± SEM	
1.Enoyl Coenzyme A hydratase, short chain, 1, mitochondrial (ECHS1)	281748	31223/8.82	7	196	2.50±0.16	<0.001
2.Cofilin-1 (CFL1)	534553	18491/8.22	7	159	2.47±0.07	<0.001
3.Glutathione transferase (GST)	281806	23598/6.89	5	339	2.44±0.08	<0.001
4.Phosphoserine aminotransferase isoform 1 (PSAT1)	533044	40340/6.60	7	166	2.25±0.09	<0.001
5. Peroxiredoxin 6 (PRDX6)	282438	25051/6.00	13	331	2.23±0.10	<0.001
6.Eukaryotic translation elongation factor 1 gamma (EEF1G)	326581	50199/6.33	8	144	2.23±0.19	<0.001
7.Triosephosphate isomerase 1 (TPI1)	281543	26673/6.45	19	507	2.19±0.20	<0.001
8.Transketolase (TKT)	445425	67728/7.20	24	341	2.13±0.10	<0.001
9.Triosephosphate isomerase 1 (TPI1)	281543	26673/6.45	10	192	2.11±0.08	<0.001
10.Enolase1 (ENO1)	281141	47296/6.37	17	385	2.08±0.09	<0.001
11.Proteasome (prosome, macropain) subunit, alpha type 1, isoform CRA_b (PSMA1)	5682	33933/6.64	6	77	2.07±0.11	<0.001
12.Ubiquitin-conjugating enzyme E2-25K (UBE2)	281225	22407/5.33	9	223	2.05±0.05	<0.001
13.Annexin A2 (ANXA2)	282689	38516/7.55	22	525	2.00±0.09	<0.001
14.Aldo-keto reductase family 1, member A1 (aldehyde reductase) (AKR1A1)	618607	36594/6.80	14	283	1.97±0.11	<0.001
15. Aconitase 2, mitochondrial (ACO2)	280976	85304/8.08	23	381	1.96±0.07	<0.001
16. Superoxide dismutase 2, mitochondrial(SOD2)	281496	24623/8.70	7	223	1.96±0.09	<0.001
17.LIM domain containing preferred translocation partner in lipoma (LPP)	524132	68216/7.87	8	98	1.94±0.10	<0.001
18. Pyruvate kinase (PKM2)	512571	61389/8.62	22	376	1.90±0.14	<0.001
19. Proteasome (prosome, macropain) subunit, alpha type 4, isoform CRA_b (PSMA4)	510423	26737/8.18	7	223	1.88±0.14	<0.001
20. Peroxiredoxin3 (PRDX3)	281998	31320/6.51	11	229	1.87±0.06	<0.001
21.PDZ and LIM domain1 (PDLIM1)	614675	35798/6.76	12	457	1.85±0.18	<0.001
22.Ribonuclease/angiogenin inhibitor 1 (RNH1)	517087	48819/4.64	6	237	1.82±0.13	<0.001
23.Transgelin 2 (TAGLN2)	282379	22412/8.39	12	189	1.77±0.13	<0.001
24.Peroxiredoxin 2 (PRDX2)	286793	21932/5.37	4	252	1.76±0.13	<0.001
25.Adenylate cyclase-associated protein 1 (CAP1)	504519	51240/7.16	13	355	1.76±0.18	<0.001

Spot #., Protein Name	GeneID	MW (Da) / PI	# Pep Matched	Protein Score	Ratio (E2/Ctl)	P-value[1]
					Mean ± SEM	
26.Zyxin (ZYX)	768226	60063/6.33	10	108	1.76±0.27	<0.001
27. Phosphoglycerate mutase 1 (PGAM1)	404148	28834/6.67	16	575	1.71±0.09	<0.001
28.Albumin (ALB)	280717	66088/5.76	25	471	1.66±0.28	<0.001
29. Eukaryotic translation elongation factor 2 (EEF2)	281138	95307/6.41	26	203	1.65±0.04	<0.001
30.Citrate synthase (CS)	280682	51740/8.16	14	409	1.57±0.06	<0.001
31.DEAD (Asp-Glu-Ala-Asp) box polypeptide 1(DDX1)	510816	82362/6.81	14	174	1.52±0.12	<0.001
32.Fascin homolog 1, actin-bundling protein (FSCN1)	507342	54751/6.55	8	115	1.47±0.07	0.002
33.Proteasome (prosome, macropain) subunit, beta type, 2 (PSMB2)	516919	22882/6.51	8	219	1.10±0.03	0.499
34. Transketolase (TKT)	445425	67728/7.20	19	164	1.06±0.04	0.685
35.ATP-dependent RNA helicase (DDX3X)	510093	73126/6.94	24	350	1.00±0.05	1.000
36.Pyruvate kinase (PKM2)	512571	61389/8.62	16	142	0.94±0.02	0.685
37. Pyruvate kinase (PKM2)	512571	61389/8.62	18	301	0.94±0.05	0.685
38.IMP (inosine monophosphate) dehydrogenase 2 (IMPDH2)	511969	55728/6.87	20	280	0.90±0.02	0.499
39.Triosephosphate isomerase 1 (TPI1)	281543	26673/6.45	18	388	0.90±0.03	0.499
40.glyceraldehyde-3-phosphate dehydrogenase (GAPDH)	281181	35845/8.50	10	106	0.87±0.04	0.380
41.Heterogeneous nuclear ribonucleoprotein A/B (hnRNPs)	513410	30634/7.68	11	175	0.86±0.02	0.345
42.Spectrin, alpha, non-erythrocytic 1 (alpha-fodrin) (SPTAN1)	540108	284401/5.20	19	89	0.83±0.02	0.252
43.Annexin A2 (ANXA2)	282689	38516/7.55	20	335	0.80±0.02	0.178
44.Transgelin (TAGLN)	513463	22584/8.87	19	295	0.79±0.02	0.158
45.Heat shock cognate 71 kDa protein (HSC70)	281831	71196/5.37	24	441	0.79±0.05	0.158
46.Heat shock 60kDa protein 1 (chaperonin) (HSP60)	511913	74985/9.05	22	461	0.74±0.03	0.081
47.Phosphoglycerate mutase 1 (PGAM1)	404148	28834/6.67	10	421	0.69±0.01	0.038
48.Hypoxia up-regulated 1 (HYOU1)	508773	111543/5.26	20	354	0.68±0.03	0.032
49.Vimentin (VIM)	280955	53667/5.02	31	689	0.66±0.01	0.023
50.Actin,beta (ACTB)	280979	40194/5.55	14	181	0.64±0.02	0.016
51.Guanine nucleotide binding protein (G protein), alpha inhibiting activity polypeptide 2 (GNAI2)	281791	40425/5.34	11	225	0.60±0.03	0.008
52.Interleukin 18 (IL18)	281249	22152/4.69	5	223	0.40±0.03	<0.001
53.Cofilin 1 (CFL1)	534553	18491/8.22	6	104	0.30±0.06	<0.001

Spot #., Protein Name	GeneID	MW (Da) / PI	# Pep Matched	Protein Score	Ratio (E2/Ctl)	P-value[1]
					Mean ± SEM	
54.Eukaryotic translation initiation factor 5A (EIF5A)	444990	16821/5.08	6	207	0.27±0.01	<0.001

[1] Statistics were performed using One Way ANOVA (Fisher LSD test), and significance was defined as $p<0.05$.

Table 2

Pathway analysis of *S-nitroso*-proteins in uterine artery endothelial cells - potential functionality.

Biological functions	**-log(p-value)**[1]	***S-nitroso*-proteins identified**[2]
Small Molecule Biochemistry	5.52-1.35	ALB*, ACO2*, AKR1A1*, ANXA2*, ECHS1*, GAPDH, GNAI2*, GST*, HSP60, IL18*, IMPDH2, LPP*, PGAM1*, PRDX2*, PRDX3*, PRDX6*, SOD2*, TKT*, TPI1*, VIM*
Cellular Assembly and Organization	4.27-1.66	ACTB*, ANXA2*, CAP1*, CFL1*, FSCN1*, GAPDH, GNAI2*, PRDX3*, SOD2*, SPTAN1, TAGLN, VIM*, HSC70, ZYX*
Molecular Transport	4.01-1.42	ALB*, EIF5A*, GAPDH, GNAII2*, HSC70, IL18*, PRDX2*, PRDX3*, PRDX6*, SOD2*, VIM*
Cell-To-Cell Signaling and Interaction	3.88-1.33	ANXA2*, CFL1*, GNAI2*, HSP60, HYOU1*, IL18*, IMPDH2, PDLIM1*, PRDX2*, PRDX3*, PRDX6*, SOD2*, SPTAN1, VIM*
Metabolism	3.53-1.35	ALB*, AKR1A1*, ANXA2*, CAP1*, CS*, ECHS1*, ENO1*, GAPDH, GNAI2*, GST*, HSP60, IL18*, IMPDH2, LPP*, PGAM1*, PKM2, PRDX2*, PRDX3*, PRDX6*, SOD2*, TKT*, TPI1*
Post-Translational Modification and Protein Folding	3.50-1.92	ALB*, ANXA2*, HSC70, HSP60, SOD2*
Cell Death	3.46-1.33	ACTB*, ALB*, CFL1*, DDX3X, EIF5A*, ENO1*, GAPDH, GST*, HSC70, HSP60, HYOU1*, IL18*, PRDX2*, PRDX3*, PRDX6*, SOD2*, UBE2K*, ZYX*
Cellular Growth and Proliferation	3.06-1.33	ACTB*, ALB*, ANXA2*, CFL1*, DDX3X, EIF5A*, ENO1*, FSCN1*, GNAI2*, GST*, HNRNPAB, HSP60, IL18*, IMPDH2, PKM2, PRDX2*, PRDX3*, PSMB2*, SOD2*, SPTAN1, VIM*, ZYX*
Cellular Movement	2.97-1.33	ACTB*, ANXA2*, CAP1*, CFL1*, DDX3X, FSCN1*, GNAI2*, HSP60, IL18*, LPP*, SOD2*, TAGLN, VIM*, ZYX*
Cell Cycle	2.52-1.32	CFL1*, DDX3X, GNAI2*, SOD2*, SPTAN1, VIM*
DNA Replication, Recombination, and Repair	2.52-1.68	CFL1*, GST*, HNRNPAB, L18*, SOD2*, VIM*
Gene Expression	2.52-1.32	ALB*, ENO1*, HNRNPAB, IL18*

[1]The significance value associated with Functional Analysis for a dataset is a measure of the likelihood that the association between a set of Functional Analysis molecules in the experiment and a given process or pathway is due to random chance. The smaller the p-value the less likely that the association is random and the more significant the association. In general, p-values less than 0.05 indicate a statistically significant, non-random association. The p-value is calculated using the right-tailed Fisher Exact Test.

[2]Protein with altered S-nitrosylation by estrogen stimulation was labeled by a "*".